COMPUTER METHODS IN APPLIED MECHANICS AND ENGINEERING 49 (1985) 109–119
NORTH-HOLLAND

DIGITAL SIMULATION OF PARALLEL INVERTERS

Y. SAITO, S. HAYANO and N. TSUYA
College of Engineering, Hosei University, Tokyo 184, Japan

H. SAOTOME
R & D Center, Fuji Electric Co. Ltd., Tokyo 191, Japan

Received 30 July 1984

Previously, a model of a nonlinear inductor exhibiting hysteresis loops was proposed, and successfully applied to typical nonlinear electric circuits [1]. This model is now generalized to include the nonlinear transformer, and applied to the digital simulation of parallel inverters. Comparison of experimental results with simulated results shows that the model taking into account the hysteresis loops behaves just like a physical inverter including the unstable operations.

0. Nomenclature

- A cross-sectional area,
- B magnetic flux density [Tesla],
- C capacitance [F],
- D mean length of flux path,
- dl infinitesimally small distance along the path D,
- E DC voltage source [V],
- f frequency [Hz],
- G conductance matrix,
- H magnetic field intensity,
- I current vector,
- I_g gate trigger current of SCR [A],
- I_h holding current of SCR [A],
- L_i nonlinear inductance [H],
- M magnetic resistance matrix,
- R_i nonlinear resistance of hysteresis [Ω],
- R_s nonlinear resistor of SCR [Ω],
- q charge [C],
- S magnetic hysteresis matrix,
- s hysteresis coefficient [Ω/m],
- t time [sec],
- V voltage vector,
- W winding matrix,
- Φ flux vector,
- ϕ magnetic flux,
- Δt stepwidth in time,
- μ permeability of magnetic material.

1. Introduction

Solid-state power control has many industrial applications, such as variable speed drives, illumination controllers and temperature regulators. Power transistors are now available with reasonably large ratings for voltage and current. Also, new semiconductor switching devices, called thyristors, have been developed with characteristics similar to those of gas-discharge tubes. These new devices are being widely used for electric power control. Advances in the fabrication of thyristors have resulted in improved reliability and lower manufacturing costs. Nowadays the thyristor has become very popular for power controllers.

A representative of the thyristors is SCR (Silicon Controlled Rectifier) which is the most widely used for electric power control devices. The SCR may be used for AC, DC power control, rectifier and inverter circuits. Hence, power electronics using SCR have been developed and practically used for various industrial devices. Since the electric power control using SCR is essentially accompanying the switching of SCR, it has been necessary to work out the mode analysis for designing the power electronic circuits [2, 3]. This mode analysis makes it difficult to develop the fully computerized design of power electronic circuits.

The authors reported that the mode analysis accompanying the design of rectifier circuits was removed by introducing the nonlinear inductor model exhibiting hysteresis loops [1]. In this paper, the nonlinear inductor model is generalized to include the transformer, and applied to single-phase parallel inverters. As a result, it is revealed that the mode analysis of inverter circuits may be removed.

At first, a model of nonlinear transformer is derived from the basic magnetic field equations. Secondly, a model of SCR is derived. Thirdly, a system of equations of the inverter is formulated by introducing the nonlinear transformer and SCR models. Finally, this system of equations is iteratively solved and its results are compared with those of experimental results.

2. Modeling of a nonlinear transformer

A magnetic field equation exhibiting hysteresis loops is given by

$$H = \left(\frac{1}{\mu}\right)B + \left(\frac{1}{s}\right)\frac{\mathrm{d}B}{\mathrm{d}t}, \tag{1}$$

where H, B, μ, s and t are the magnetic field intensity, magnetic flux density, permeability, hysteresis coefficient and time, respectively. In (1), the permeability μ is a single-valued function of B representing the saturation property; also, the hysteresis coefficient s is a single-valued function of $\mathrm{d}B/\mathrm{d}t$ representing the hysteresis property of iron. For further details of (1), you may refer to [1, 4–6].

In order to derive the nonlinear transformer model, let us consider a transformer shown in Fig. 1(a). By considering (1) and Fig. 1(a), it is possible to write the following relation:

$$\int_0^D H\,\mathrm{d}l = \int_0^D \left[\left(\frac{1}{\mu}\right)B + \left(\frac{1}{s}\right)\frac{\mathrm{d}B}{\mathrm{d}t}\right]\mathrm{d}l, \tag{2}$$

where D and $\mathrm{d}l$ denote the mean length of the magnetic flux path and an infinitesimally small distance along the flux path D, respectively. With A denoting the cross-sectional area normal to the flux path, the relationship between the magnetic flux density B and magnetic flux ϕ is given by

$$B = \phi/A. \tag{3}$$

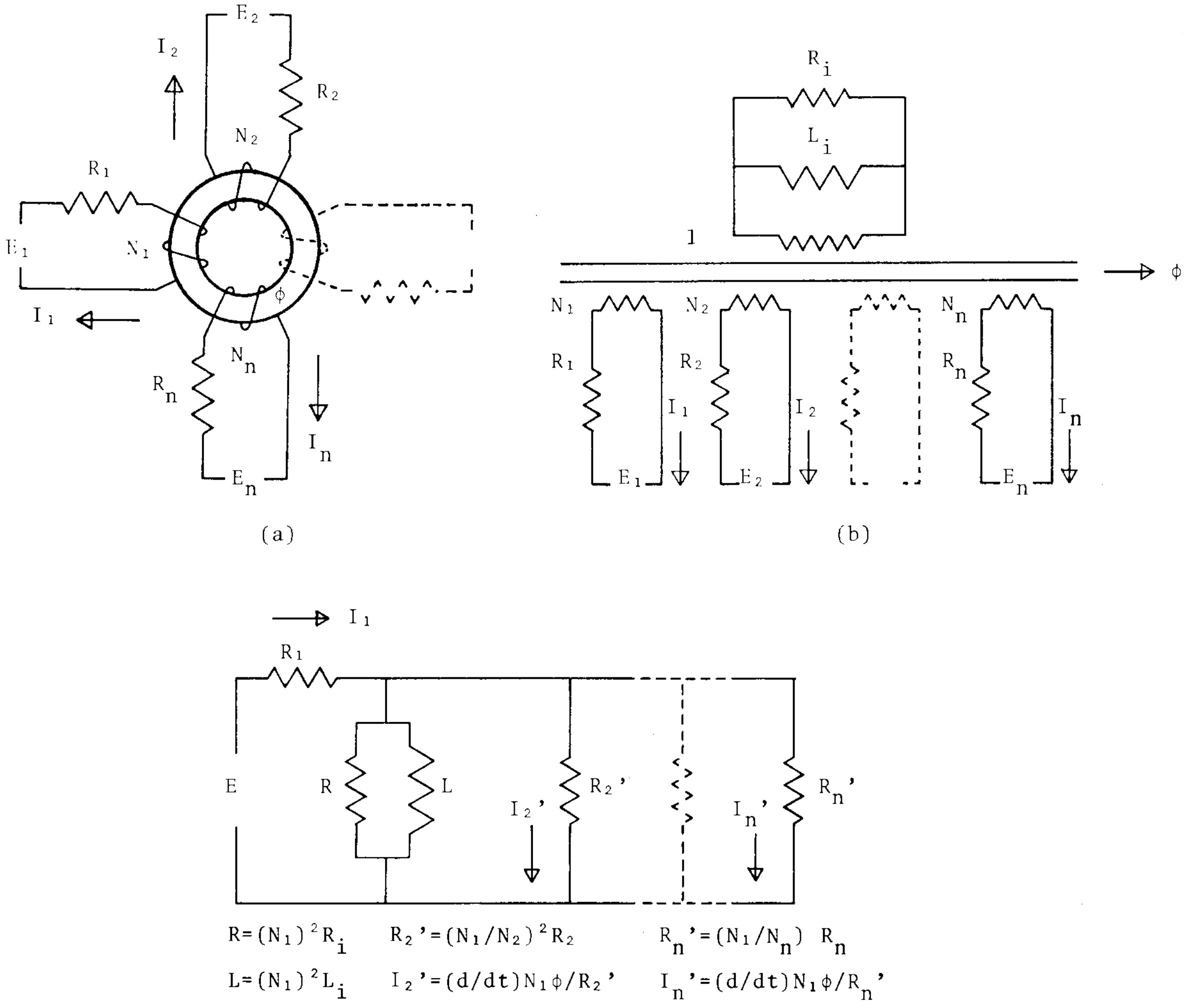

Fig. 1. (a) Schematic diagram of a transformer, where the mean length of magnetic flux path and cross-sectional area are D and A, respectively. (b) Circuit model of nonlinear transformer. (c) Equivalent circuits of nonlinear transformer.

By means of (3), the right-hand term in (2) is rewritten by

$$\int_0^D \left[\left(\frac{1}{\mu}\right)B + \left(\frac{1}{s}\right)\frac{\mathrm{d}B}{\mathrm{d}t}\right]\mathrm{d}l = \left(\frac{1}{L_i}\right)\phi + \left(\frac{1}{R_i}\right)\frac{\mathrm{d}\phi}{\mathrm{d}t}, \tag{4}$$

where the inductance L_i and resistance R_i are defined by

$$L_i = \mu\,(A/D)\,, \tag{5}$$

$$R_i = s(A/D)\,. \tag{6}$$

Since the magnetic flux ϕ is related to the magnetic flux density B by (3), the inductance L_i and resistance R_i in (5), (6) are formally expressed as

$$L_i = f(\phi), \tag{7}$$

$$R_i = f\left(\frac{d\phi}{dt}\right), \tag{8}$$

where $f(*)$ denotes a single-valued function of $*$.

On the other hand, the left-hand term of (2) is rewritten in terms of the current vector I and winding matrix W, that is,

$$\int_0^D H\,dl = W^t I, \tag{9}$$

where I and W are

$$I = \{I_1, I_2, \ldots, I_n\}, \tag{10}$$

$$W = [N_1, N_2, \ldots, N_n]^t. \tag{11}$$

The currents $I_1, I_2, \ldots, I_n$ in (10), the number of turns of coil $N_1, N_2, \ldots, N_n$ in (11) are shown in Fig. 1(a); and the superscript t in (11) refers to the transposed matrix. Substituting (4) and (9) into (2) yields

$$W^t I = \frac{\phi}{L_i} + \frac{d\phi/dt}{R_i}. \tag{12}$$

By considering Fig. 1(a), it is found that the current vector I in (12) can be rewritten by

$$I = G[V - W(d/dt)\phi], \tag{13}$$

where the conductance matrix G and voltage vector V are given by

$$G = \lceil 1/R_1, 1/R_2, \ldots, 1/R_n \rfloor. \tag{14}$$

$$V = \{E_1, E_2, \ldots, E_n\}. \tag{15}$$

In (14) and (15), the resistances $R_1, R_2, \ldots, R_n$ and voltages $E_1, E_2, \ldots, E_n$ are shown in Fig. 1(a). By means of (12)–(15), it is possible to draw the circuit model of the nonlinear transformer as shown in Fig. 1(b), where the transformer shown in Fig. 1(b) is an ideal transformer. In order to compare this circuit model with a conventional one, let us assume that the voltages $E_2, E_3, \ldots, E_n$ in (15) are set to zero; then by substituting (13)–(15) into (12) and rearranging, we can obtain the following relation:

$$\frac{E_1}{R_1} = \left[\left(\frac{1}{R_1}\right) + \left(\frac{N_2}{N_1}\right)^2\left(\frac{1}{R_2}\right) + \cdot\cdot\cdot + \left(\frac{N_n}{N_1}\right)^2\left(\frac{1}{R_n}\right) + \left(\frac{1}{N_1}\right)^2\left(\frac{1}{R_i}\right)\right](\mathrm{d}/\mathrm{d}t)N_1\phi$$
$$+ \left(\frac{1}{N_1}\right)^2\left(\frac{1}{L_i}\right)N_1\phi\,. \tag{16}$$

Equation (16) yields the equivalent circuit of the nonlinear transformer as shown in Fig. 1(c). When leakage inductances are neglected in the conventional equivalent circuit of transformer, then the conventional equivalent circuit reduces to the same form as Fig. 1(c) [7]. Moreover, when the resistances $R_2, R_3, \ldots, R_n$ in (16) are set to an infinitely large value, then (16) reduces to the nonlinear inductor model exhibiting hysteresis loops [1].

3. Modeling of SCR

Generally, the modeling of SCR is one of the difficult problems in computerized electronic circuit design [8], because SCR is a complex-structured semiconductor. Furthermore, there are a lot of different types of structures. Therefore, in this paper, SCR is modeled as a simple nonlinear resistor R_s that is a function of the terminal voltage as well as the gate trigger pulse current I_g. The forward voltage vs. current characteristic of SCR is, for example, assumed to be like that of a diode while the gate current I_g takes a reasonable value. Thus, it is assumed that the forward voltage vs. current characteristic of SCR is represented by a simple hyperbola. Also, the backward resistance of SCR is assumed to take a quite large value. Fig. 2 shows the flow chart of the SCR function.

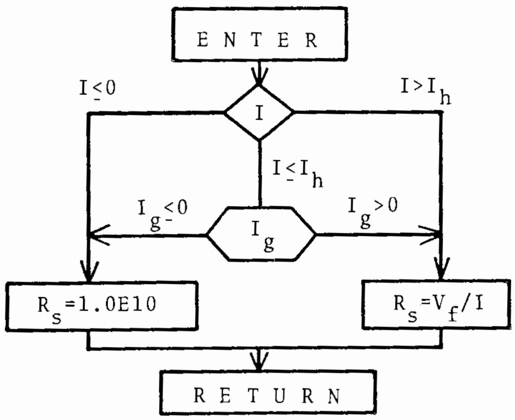

Fig. 2. Flow chart of the SCR function.

4. A system of equations for a single-phase parallel inverter

Fig. 3(a) shows the schematic diagram of a single-phase parallel inverter, and Fig. 3(b) shows the circuit model of this inverter which is derived by means of the nonlinear transformer

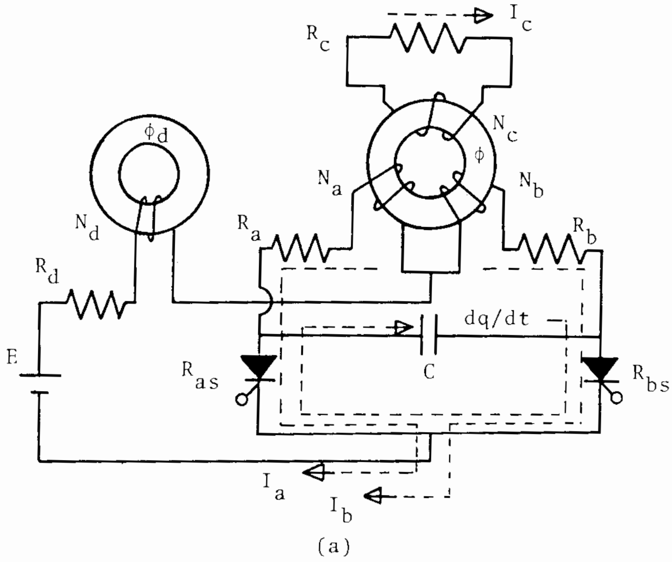

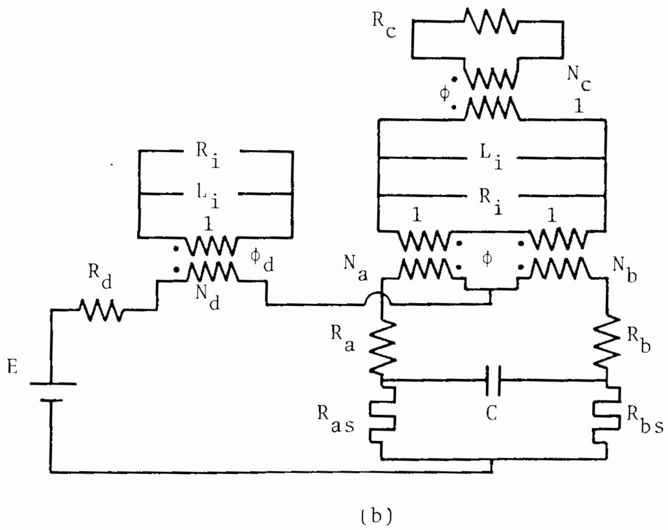

Fig. 3. (a) Schematic diagram of a parallel inverter. (b) Circuit model of a parallel inverter.

and SCR models. A system of equations for this inverter is best expressed in matrix notation involving the voltage vector V, current vector I, conductance matrix G, winding matrix W and flux vector Φ, viz.,

$$I = G[V - W(\mathrm{d}/\mathrm{d}t)\Phi], \tag{17}$$

where

$$V = \{E, E, 0\}, \tag{18}$$

$$I = \{I_a, I_b, I_c\}, \tag{19}$$

$$\Phi = \{\phi_d, \phi_s, q\}, \tag{20}$$

$$G = \begin{vmatrix} R_d + R_a + R_{as} & R_d & 0 \\ R_d & R_d + R_b + R_{bs} & 0 \\ 0 & 0 & R_c \end{vmatrix}^{-1}, \tag{21}$$

$$W = \begin{vmatrix} N_d & N_a & R_{as} \\ N_d & -N_b & -R_{bs} \\ 0 & N_c & 0 \end{vmatrix}. \tag{22}$$

As shown in Fig. 3, E in (18) denotes the DC voltage source; I_a, I_b, I_c in (19) denote the loop currents; ϕ_d, ϕ_s, q in (20) denote the loop magnetic flux in the DC reactor, loop magnetic flux in the transformer and charge in the inverting capacitor; R_a, R_b, R_c, R_d in (21) denote the resistances of the transformer, load and DC reactor; N_a, N_b, N_c, N_d in (22) denote the number of turns of coils wound to the transformer and DC reactor, respectively. As shown in Fig. 3(b), the nonlinear resistors of SCR are denoted by R_{as} and R_{bs}. Moreover, the superscript -1 refers to the inversed matrix.

Multiplication of the matrix W^t to the current vector I gives

$$W^t I = M\Phi + S(\mathrm{d}/\mathrm{d}t)\Phi, \tag{23}$$

where

$$M = \begin{vmatrix} 1/L_i & 0 & 0 \\ 0 & 1/L_i & 0 \\ 0 & 0 & -1/C \end{vmatrix}, \tag{24}$$

$$S = \begin{vmatrix} 1/R_i & 0 & 0 \\ 0 & 1/R_i & 0 \\ 0 & 0 & -R_{as} - R_{bs} \end{vmatrix}. \tag{25}$$

The inductance L_i in (24) and resistance R_i in (25) are the same as those of (12); and the inverting capacitor C in (24) is shown in Fig. 3. By substituting (17) into (23) and rearranging, the system of equations which must be solved for the flux vector Φ is given by

$$(\mathrm{d}/\mathrm{d}t)\Phi = [S + W^t G W]^{-1}[-M\Phi + W^t G V]. \tag{26}$$

5. Numerical method of solution

As shown in (7) and (8), the inductance L_i and resistance R_i are respectively the functions of magnetic flux ϕ and the time derivative of magnetic flux $\mathrm{d}\phi/\mathrm{d}t$. Furthermore, the terminal voltage of SCR depends on the flux vector Φ, the time derivative of the flux vector $(\mathrm{d}/\mathrm{d}t)\Phi$ and the gate trigger current I_g. Thereby, (26) is formally expressed as

$$(\mathrm{d}/\mathrm{d}t)\Phi = F[\Phi, (\mathrm{d}/\mathrm{d}t)\Phi, I_g]. \tag{27}$$

Equation (27) means that the circuit model of a single-phase parallel inverter yields a system of nonlinear differential equations whose parameters are functions of the flux vector Φ, the time derivative of the flux vector $(\mathrm{d}/\mathrm{d}t)\Phi$ and the gate trigger current I_g. For solving (27) numerically, this system of equations is replaced by the following divided differences:

$$\frac{\Phi_{t+\Delta t} - \Phi_t}{\Delta t} = F\left[\frac{\Phi_{t+\Delta t} + \Phi_t}{2}, \frac{\Phi_{t+\Delta t} - \Phi_t}{\Delta t}, I_g\right], \tag{28}$$

where Δt denotes the stepwidth in time; subscripts $t + \Delta t$ and t refer to the time $t + \Delta t$ and t, respectively. With the superscripts $[K+1]$, $[K]$, $[K-1]$ denoting the number of iterations, (28) is iteratively solved by

$$\Phi_{t+\Delta t}^{[K+1]} = \Phi_t + \Delta t F\left[\frac{\Phi_{t+\Delta t} + \Phi_t}{2}, \frac{\Phi_{t+\Delta t}^{*} - \Phi_t}{\Delta t}, I_g\right], \tag{29}$$

where $\Phi_{t+\Delta t}^{*}$ is given by

$$\Phi_{t+\Delta t}^{*} = \Phi_{t+\Delta t}^{[K-1]} + 0.5(\Phi_{t+\Delta t}^{[K]} - \Phi_{t+\Delta t}^{[K-1]}). \tag{30}$$

6. Numerical solutions

Various constants used in the simulations of the single-phase parallel inverter are listed in Table 1. Also, the magnetization curves used in the simulations are shown in Fig. 4, and they are introduced by linear interpolation in the simulations.

By means of several numerical tests, it is revealed that the stepwidth Δt in (28)–(30) must be smaller than or equal to 0.25[msec] while the convergence and accuracy of the solutions are taken into account.

At first, we checked up the stable frequency range of the inverter. As a result, the tested inverter showed an interesting feature on the low-frequency limit. As shown in Fig. 5, the low

Table 1
Various constants used in the simulations

Number of turns of DC coil	N_d	600	[turns]
Number of turns of primary coil (a)	N_a	300	[turns]
Number of turns of primary coil (b)	N_b	300	[turns]
Number of turns of secondary coil	N_c	300	[turns]
Electric resistance of DC coil	R_d	3.15	[Ω]
Electric resistance of coil (a)	R_a	1.36	[Ω]
Electric resistance of coil (b)	R_b	1.32	[Ω]
Electric resistance of secondary coil	R_c	101.8	[Ω]
On state voltage drop of SCR	V_f	1.6	[V]
Holding current of SCR	I_h	0.06	[A]
DC source voltage	E	20	[V]

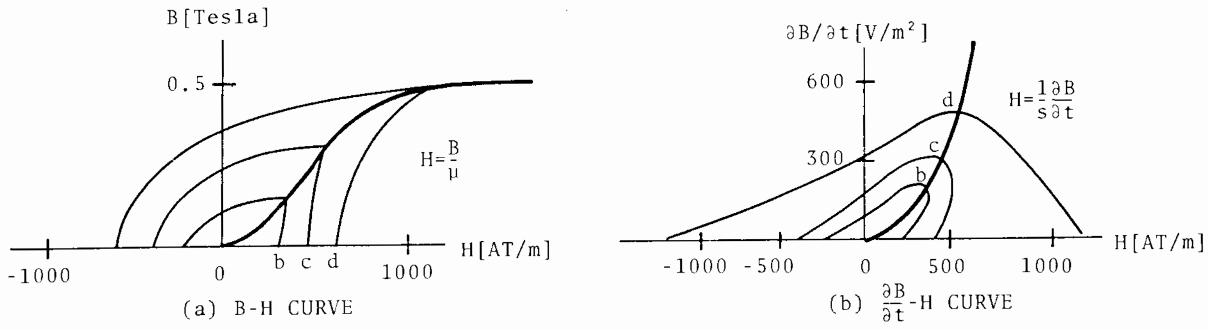

Fig. 4. Magnetization curves used in the simulations.

frequency unstable region spreads like a tree. In order to demonstrate the validity of the simulation model, we applied our simulation model to this low-frequency unstable region. The simulation results are also shown in Fig. 5.

Secondly, the simulations were carried out to the steady-state characteristics of the inverter, and the results were shown in Fig. 6 together with the experimental results.

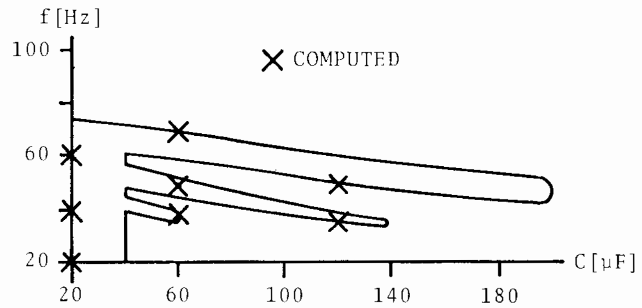

Fig. 5. Low-frequency unstable region, where $\Delta t = 0.1$ [msec].

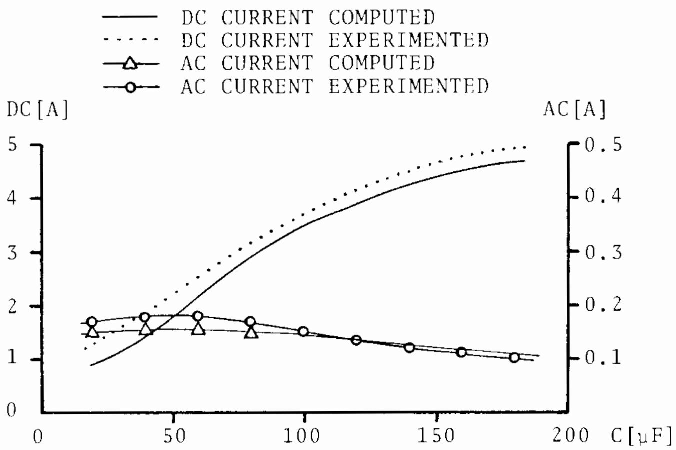

Fig. 6. Steady-state DC and AC currents, where $f = 100$ [Hz] and $\Delta t = 0.25$ [msec].

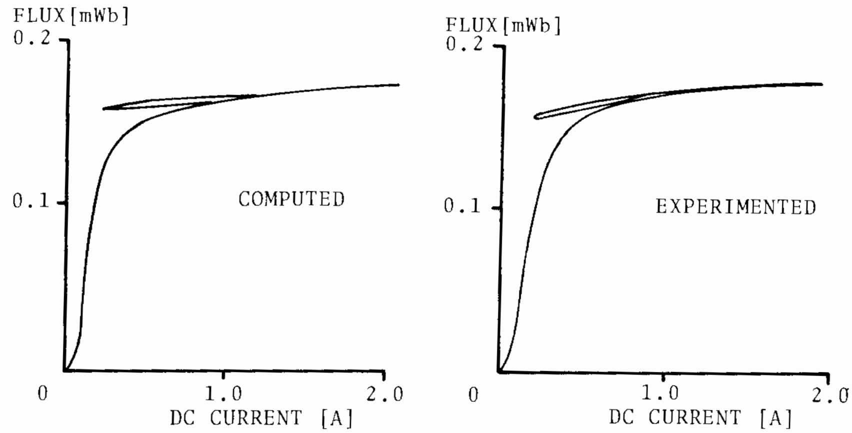

Fig. 7. Transient magnetization of DC reactor, where $f = 100$ [Hz], $C = 20$ [μF] and $\Delta t = 0.25$ [msec].

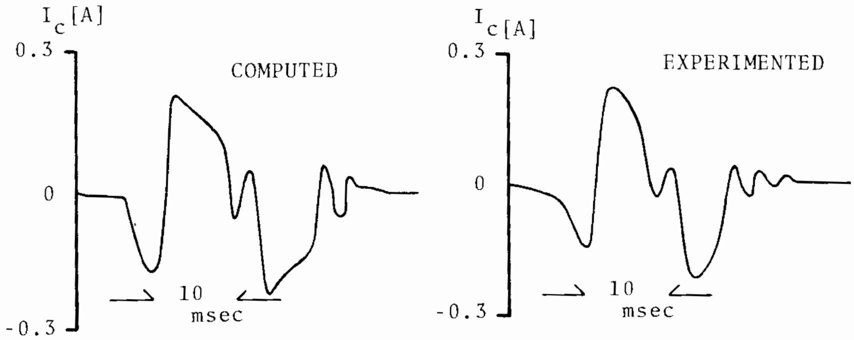

Fig. 8. Transient output AC current under the case of fault in the inversion, where $f = 49$ [Hz], $C = 60$ [μF] and $\Delta t = 0.1$ [msec].

Finally, the simulations were carried out to the transient characteristics of the inverter. Fig. 7 shows a transient magnetization characteristic of DC reactor under the stable operation; also Fig. 8 shows a transient output AC current under the unstable operation.

7. Conclusions

As shown above, we have derived the nonlinear transformer model and applied to the digital simulation of the single-phase parallel inverter. Since our simulation model of the inverter takes into account the full of nonlinearities of the magnetization material as well as resistance of SCR, it is found that the simulation model is able to simulate the unstable behaviors of the inverter.

The authors plan to use this simulation model to the inverters utilizing a new magnetic material [9]. The time required to obtain the results of Fig. 7 was about 3 hours on the Micro-Computer (Z80A CPU).

References

[1] Y. Saito, H. Saotome and T. Yamamura, A lumped circuit model for a nonlinear inductor exhibiting dynamic hysteresis loops and its application to the electric circuits, Comput. Meths. Appl. Mech. Engrg. 38 (2) (1983) 185–202.
[2] B.M. Bird and K.G. King, An Introduction to Power Electronics (Wiley, New York, 1983).
[3] M.A. Slonim and P.P. Biringer, Analysis of the transient and steady-state processes in the parallel inverter, IEEE Trans. Industrial Electronics 29 (4) (1982) 329–336.
[4] Y. Saito, Three-dimensional analysis of nonlinear magnetodynamic fields in electromagnetic devices taking into account the dynamic hysteresis loops, IEEE Trans. Magnetics 18 (2) (1982) 546–551.
[5] Y. Saito, H. Saotome, S. Hayano and T. Yamamura, Modeling of hysteretic and anisotropic magnetic field problems, IEEE Trans. Magnetics 19 (6) (1983) 2510–2513.
[6] Y. Saito, S. Hayano, T. Yamamura and N. Tsuya, A representation of magnetic hysteresis, IEEE Trans. Magnetics 20 (5) (1984) 1434–1436.
[7] A.E. Fitzgerald, C. Kingsley and A. Kusko, Electric Machinery (McGraw-Hill, New York, 1971).
[8] R.L. Avant, F.C.Y. Lee and D.Y. Chen, A practical SCR model for computer aided analysis of AC resonant charging circuits, IEEE Trans. Industrial Electronics 29 (4) (1982) 319–329.
[9] K.I. Arai and N. Tsuya, Ribbon-form silicon-iron alloy containing around 6.5 percent silicon, IEEE Trans. Magnetics 16 (1) (1980) 126–129.